1 **Electronic supplementary information**

2 **Plasmid Binding to Metal Oxide Nanoparticles Inhibited Lateral Transfer of Antibiotic**

3 **Resistance Genes**

4 Xiaojie Hu, [a] Bing Yang, [a] Wei Zhang, [b] Chao Qin, [a] Xue Sheng, [a] Patryk Oleszczuk, [c] and

5 Yanzheng Gao [a],*

6 [a] Institute of Organic Contaminant Control and Soil Remediation, College of Resources and

7 Environmental Sciences, Nanjing Agricultural University, Nanjing 210095, P.R. China.

8 [b] Department of Plant, Soil and Microbial Sciences, and Environmental Science and Policy

9 Program, Michigan State University, East Lansing, Michigan 48824, United States.

10 [c] Department of Environmental Chemistry, University of Maria Skłodowska-Curie, Lublin 20-

11 031, Poland.

12

13 **Corresponding author:** Yanzheng Gao, Address: Weigang Road 1, Nanjing 210095, China.

14 Tel: +86-25-84395019. ORCID No.: 0000-0002-3814-3555. E-mail: gaoyanzheng@njau.edu.cn.

15

16

17

18 **CONTENT:**

19 **S1. Supplemental methods**

20 **S2. Supplemental results**

21 **References**

22

S1. Supplemental methods

AFM, SEM, TEM, and FTIR analysis.

AFM. The mixtures of plasmids and MONPs were equilibrated at 25°C and 200 rpm for 2 hours. Afterwards, 20 µL was deposited on a mica surface and dried under nitrogen gas for 20 minutes. Images of plasmid samples were then obtained by AFM (Dimension Fast Scan; Bruker, Karlsruhe, Germany).

SEM and TEM. After mixing at 25°C and 200 rpm for 2 hours, the plasmid and MONP suspensions were transferred into the culture of competent cells, followed by the same transformation procedure described in the manuscript. The obtained bacterial suspensions were centrifuged at 6,000 rpm at 25°C and washed several times to remove residual LB medium. Glutaraldehyde solution (2.5%) was applied to fix bacterial cells. The cells were dehydrated through a graded ethanol series, and then coated with gold for SEM (S-3400N; Hitachi, Tokyo, Japan) or placed onto a carbon-coated copper grid for TEM (JEM-2100; JEOL, Tokyo, Japan).

FTIR. The plasmids and MONPs were mixed at 25°C and 200 rpm for 2 hours and then freeze-dried, followed by mixing with KBr on a mass ratio of 1:100 before analysis using a FTIR spectrometer (Nicolet NEXUS870; Thermo Scientific).

Model computation.

Computational settings. The generalized gradient approximation (GGA) with the Perdew, Burke, and Enzerhof (PBE) functional parameters were employed to conduct the model computation,[1] as carried out in the DMol3 module of the Materials Studio package (Accelrys Software Inc., San Diego, USA).[2] The geometrical and electronic structures of nanoparticle-base or nanoparticle-phosphate backbone complexes were computed in periodic boundary conditions (PBC) in density functional theory (DFT) computation. The global orbital cutoff (fine standard in DMol3) was set

46   at 4.8 Å. The water solvent environment was modeled by applying the conductor-like screening

47   model (COSMO),[3] and the medium quality mesh size was used for numerical integration. A 1×1

48   $\times 1$ Monkhorst-Pack k-point grid was used to select the Brillouin zone for the structural

49   optimization. Convergence efficiency was improved by a Fermi smearing of 0.005 hartree (Ha).[4]

50   **Computational model.** The geometries of the phosphate backbone and four bases of DNA were

51   structured in ChemBioOffice Software (CambridgeSoft, Cambridge, USA), and the optimized

52   geometries were calculated by Gaussian 09 with use of the B3LYP/6-311G (d, p) basis sets. The

53   supercells of Al_2O_3NP, ZnONP, and TiO_2NP were optimized, and the calculated lattice constants

54   were 1) a = 16.486 Å, c = 37.916 Å, 2) a = 15.616 Å, c = 36.596 Å, and 3) a = 14.795 Å, and c =

55   39.745 Å, respectively. The most stable surface among the three cleavage planes of α-Al_2O_3 (0 0

56   1), ZnO (0 1 0), and TiO_2 (1 1 0) surface[5-7] was used in this study. The vacuum thickness was set

57   at 30 Å that was normal to the used surface with the intention to remove fake interactions between

58   the adsorbate and the periodic image of the bottom layer. Surface hydrogenation of Al_2O_3NP and

59   TiO_2NP will occur and reactive surface sites are formed.[6, 7] The test calculations with a larger

60   orbital cutoff (5.2 Å) and denser k-point sampling ($2 \times 2 \times 1$) showed no alteration in energetic or

61   structural properties. These tests confirmed that the settings and models for model computation in

62   our experiment were credible enough to express the attributes of the phosphate backbone and four

63   bases of DNA on the surfaces of MONPs. The weak interaction between molecules was mainly

64   analyzed by the Independent Gradient Model method.[8] Results were analyzed using VMD 1.93

65   software, Multiwfn Analyzer,[9] and Origin 2016 software.

66

S2. Supplemental results

Table S1. General properties of test metal oxide nanoparticles in this study.

Particles	Average primary particle diameter (nm)	Hydrodynamic[a] diameter (nm)	Zeta potential in[a] deionized water (mV)	Purity (%)
ZnONP	30 ± 10	102.40 ± 4.67	-12.27 ± 1.50	99.9
Al_2O_3NP	30	110.06 ± 20.14	8.85 ± 1.23	99.9
TiO_2NP (Rutile)	50 ± 10	198.60 ± 19.09	-19.80 ± 0.72	99.8

[a] Hydrodynamic diameter and zeta potential of MONPs (100 mg L^{-1}) were both determined in deionzed water using Malvern Zetasizer nano series-Nano ZS90.

Table S2. Properties of metal oxide nanoparticles after binding with plasmids.

Particles	Hydrodynamic[b] diameter (nm)	Zeta potential in[b] deionized water (mV)
ZnONP	190.90 ± 0.99	-16.10 ± 0.71
Al_2O_3NP	812.60 ± 110.17	-19.17 ± 1.93
TiO_2NP (Rutile)	651.63 ± 65.53	-20.33 ± 0.15

[b] Hydrodynamic diameter and zeta potential of MONPs (100 mg L^{-1}) binding with pUC19 plasmid (25 ng, at 200 rpm, 25℃, 2 h) were both determined in deionzed water by using Malvern Zetasizer nano series-Nano ZS90.

77 **Table S3.** The identifiable infrared spectral features of plasmid DNA without reacting with
78 MONPs and their corresponding functional groups.

Wavenumber (cm⁻¹)	Functional groups	References
1,064.9	stretching vibration of P-O	10
1,238.3	dissymmetrical stretch vibration of PO_2^-	10
1,483.5	cytosine (C)	11
1,606.2	adenine (A)	11
1,649.0	thymine (T)	11
1,693.2	guanine (G)	11
less than 900.0	"fingerprint" zone	10

79

80

81 **Figure S1.** Transmission electron microscope images of ZnONP (**a**), Al_2O_3NP (**b**), and TiO_2NP
82 (**c**). MONP solutions were prepared in deionized water and sonicated for 20 minutes in an
83 ultrasonic bath to disperse the particles. The solution was then added onto a copper grid coated
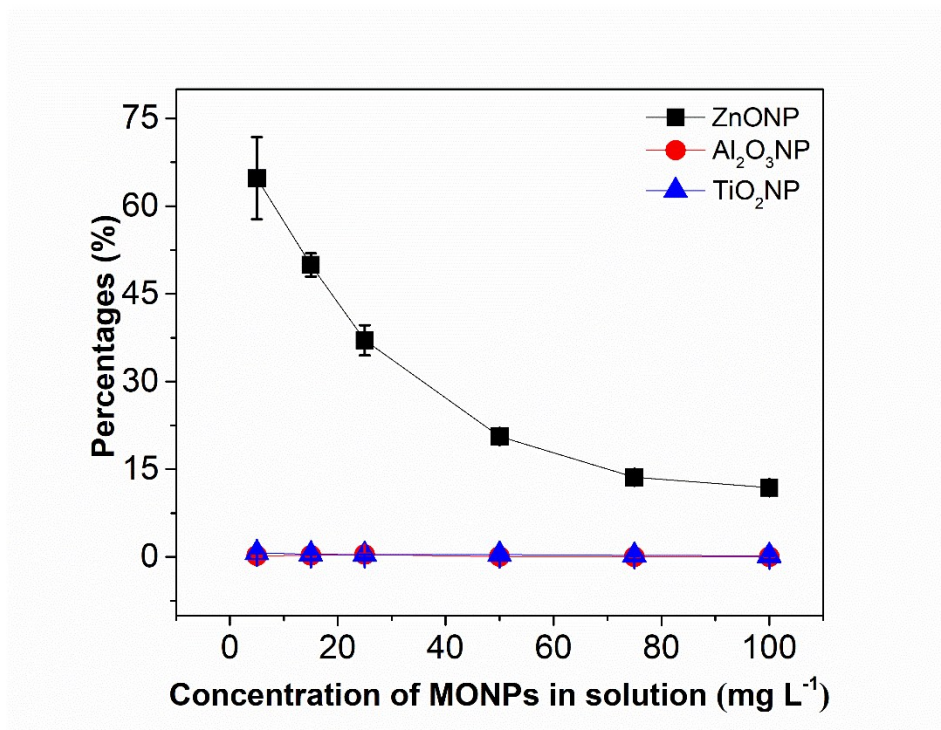84 with carbon to get TEM images (JEM-2100; JEOL, Tokyo, Japan).
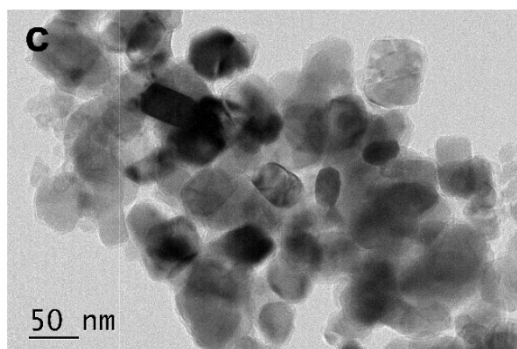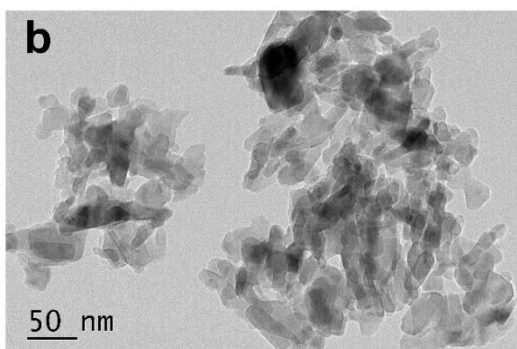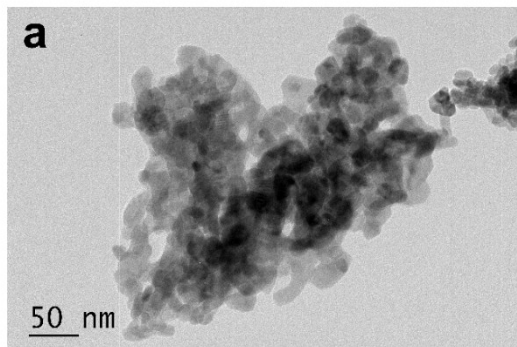
85
86

87 **Figure S2**. Percentages of metal ions released from ZnONP, Al$_2$O$_3$NP, and TiO$_2$NP in deionized
88 water at pH 7.0 at 25°C. The percentages of metal ions dissolved from MONPs were calculated as
89 follows:

90 $$Percentages~(\%) = \frac{molar~mass~of~dissolved~metal~ions~in~solution}{molar~mass~of~metal~element~in~MONPs} \times 100~\%$$


91
92

93 **Figure S3.** AFM images of TiO_2NP after reacting with the pUC19 plasmid. The mixtures of
94 plasmid and TiO_2NP were incubated at 200 rpm at 25°C for 2 hours, and then 20 μL was deposited
95 on a mica surface and dried under nitrogen gas for 20 minutes. The images of plasmid samples
96 were obtained by AFM (Dimension Fast Scan; Bruker, Karlsruhe, Germany).

97

98
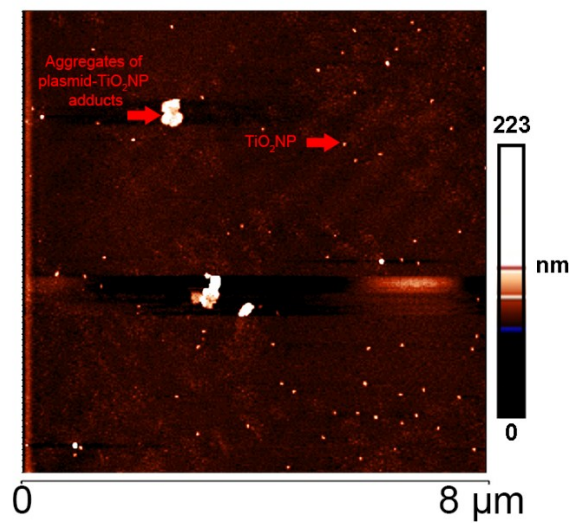
Figure S4. FTIR analysis of ZnONP (**a**), Al$_2$O$_3$NP (**b**), and TiO$_2$NP (**c**) before and after binding with the pUC19 plasmid. FTIR analysis of MONPs in the absence or presence of plasmid was conducted as follows: The MONP solutions with or without plasmids were incubated at 200 rpm at 25°C for 2 hours and then freeze-dried. After mixing with KBr (mass ratio of 1:100), the samples were analyzed by a Nicolet NEXUS870 FTIR spectrometer (Thermo Scientific).
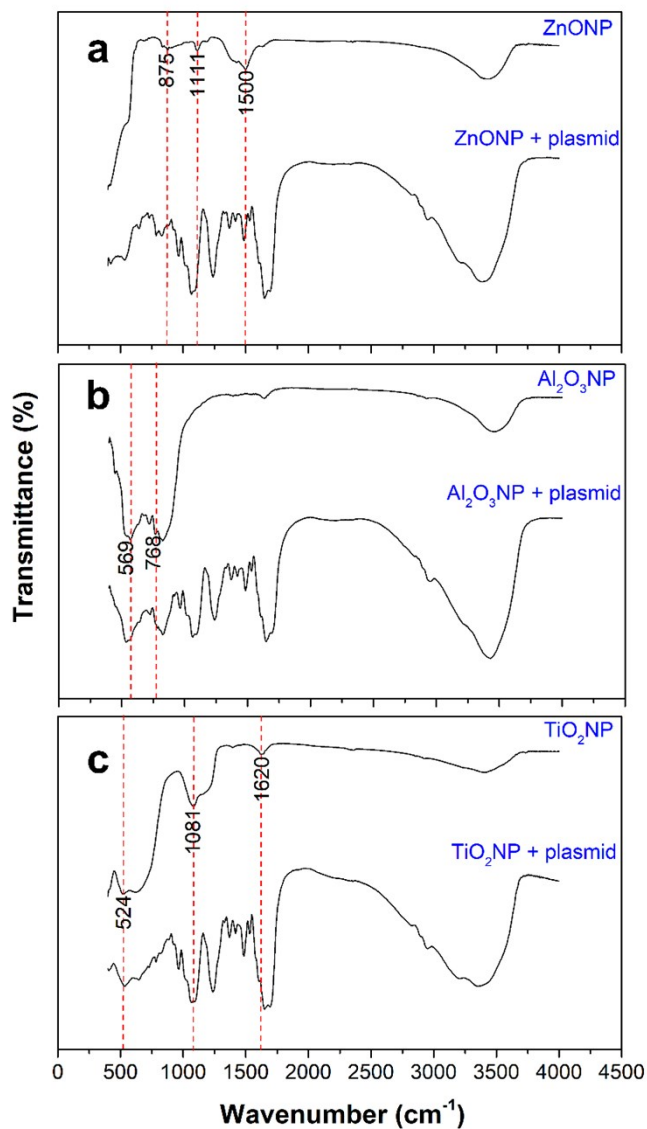
REFERENCES

1. J. P. Perdew, K. Burke and M. Ernzerhof, Generalized gradient approximation made simple, *Phys. Rev. Lett.*, 1996, **77**, 3865−3868.

2. B. Delley, An all-electron numerical method for solving the local density functional for polyatomic molecules, *J. Chem. Phys.*, 1990, **92**, 508−517.

3. A. Klamt, Conductor-like screening model for real solvents: A new approach to the quantitative calculation of solvation phenomena, *J. Phys. Chem.*, 1995, **99**, 2224−2235.

4. B. Delley, in *Theoretical and Computational Chemistry*, eds. J. M. Seminario and P. Politzer, Elsevier, 1995, vol. 2, pp. 221−254.

5. Q. Yuan, Y. P. Zhao, L. Li and T. Wang, Ab initio study of ZnO-based gas-sensing mechanisms: Surface reconstruction and charge transfer, *J. Phys. Chem. C*, 2007, **113**, 6107−6113.

6. J. D. Kubicki, A. V. Bandura and D. G. Sykes, Adsorption of Water on the TiO_2 (Rutile) [110] Surface: A DFT Study, 2004.

7. M. Zhang, G. He and G. Pan, Structure and stability of arsenate adsorbed on α-Al_2O_3 single-crystal surfaces investigated using grazing-incidence EXAFS measurement and DFT calculation, *Chem. Geol.*, 2014, **389**, 104−109.

8. C. Lefebvre, G. Rubez, H. Khartabil, J. C. Boisson, J. Contreras-García and E. Hénon, Accurately extracting the signature of intermolecular interactions present in the NCI plot of the reduced density gradient versus electron density, *Phys. Chem. Chem. Phys.*, 2017, **19**, 17928−17936.

127 9.   T. Lu and F. Chen, Multiwfn: A multifunctional wavefunction analyzer, *J. Comput. Chem.*,

128   2012, **33**, 580−592.

129 10.   C. Qin, F. Kang, W. Zhang, W. Shou, X. Hu and Y. Gao, Environmentally-relevant

130   concentrations of Al(III) and Fe(III) cations induce aggregation of free DNA by

131   complexation with phosphate group, *Water Res.*, 2017, **123**, 58−66.

132 11.   D. K. Jangir, G. Tyagi, R. Mehrotra and S. Kundu, Carboplatin interaction with calf-

133   thymus DNA: A FTIR spectroscopic approach, *J. Mol. Struct.*, 2010, **969**, 126−129.

134